Deterministic aspects of Nonlinear Modulation Instability

E van Groesen, Andonowati & N. Karjanto

Applied Analysis & Mathematical Physics, University of Twente,
POBox 217, 7500 AE, Netherlands
& Jurusan Matematika, Institut Teknologi Bandung,
Jl. Ganesha 10, Bandung Indonesia
groesen@math.utwente.nl, aantrav@attglobal.net,
n.karjanto@math.utwente.nl

Abstract. Different from statistical considerations on stochastic wave fields, this paper aims to contribute to the understanding of (some of) the underlying physical phenomena that may give rise to the occurence of extreme, rogue, waves. To that end a specific deterministic wavefield is investigated that develops extreme waves from a uniform background. For this explicitly described nonlinear extension of the Benjamin-Feir instability, the soliton on finite background of the NLS equation, the global down-stream evolving distortions, the time signal of the extreme waves, and the local evolution near the extreme position are investigated. As part of the search for conditions to obtain extreme waves, we show that the extreme wave has a specific optimization property for the physical energy, and comment on the possible validity for more realistic situations.

Keywords: rogue waves, modulational instability, deterministic extreme waves, constrained minimal energy principle.

1 Introduction

In this contribution we describe various aspects related to modulational, Benjamin-Feir, instability that have been found in a detailed study of a family of wavefields. These aspects give rise to some understanding of phenomena that are observable in the downstream evolution of unidirectional waves, showing the spatial evolution from a slightly modulated uniform wave train to a position where large amplitude amplification occurs and extreme waves arise. Although these findings are for a special class of solutions in a simplified model, it is expected that at least some of the phenomena and underlying physics could be quite characteristic for more general situations in which extreme ('rogue') waves are observed. This is to be expected, since the family of wavefields studied are the deterministic description of the fully nonlinear evolution of the initially linear Benjamin-Feir instability with one pair of unstable sidebands. This family is known in the NLS model as the Soliton on Finite Background (SFB), given in [1]. Some of the results reported in detail in Andonowati e.a., [2], will be put in a broader perspective and, where possible, a link with research on stochastic elements will be

made. In fact, different from the statistical approach that envisages the occurrence of extreme waves as a very rare occasion for which it is not yet known if there are special circumstances that give rise to their occurrence, we start from the opposite direction: what are the basic underlying physical properties of extreme waves (as they appear in this family), and extract information from this that may be characteristic for more realistic cases too.

Slowly varying evolutions of a monochromatic wave with wavenumber and frequency (k_0, ω_0) satisfying the dispersion relation, are described in first order of the (small) wave elevations with a complex valued amplitude A like

$$\eta(x,t) \approx A \exp\left[i\left(k_0 x - \omega_0 t\right)\right] + cc$$

To study the spatial evolution, it is practical to describe the amplitude in variables with delayed time, with the delay determined by the corresponding group velocity V_0, so $\xi = x, \tau = t - x/V_0$, where (x,t) are the (scaled) physical laboratory variables (we suppress the first order and second order scaling coefficients in τ and ξ respectively, just as we do in the amplitude). To incorporate dispersive and nonlinear effects in comparable order, A should satisfy in the lowest nontrivial approximation the NLS equation, given by

$$\partial_\xi A = -i\left[\beta\partial_\tau^2 A + \gamma|A|^2 A\right]$$

where β, γ are constants, depending on the monochromatic wave. For sufficiently large wavenumbers, both parameters have the same sign (positive say, without restriction since the sign of ξ can be changed). Then dispersive effects (broadening of linear wavegroups) can be balanced by focussing effects from nonlinearity; in this paper we consider only this case, the 'deep water limit'.

In section 2 we present the basic observations of the family of SFB[1]. We first present a description of the complete spatial evolution, using the envelope of the waves to illustrate the development of wavegroups, and the maximal temporal amplitude to depict the largest possible surface elevations at each point. We investigate the time signal, and its spectral properties, at the extreme position where the largest waves appear and describe how, as a consequence of the appearance of phase singularities, waves in one wavegroup are distinguished between extreme and intermittent waves that have opposite phase. Near the extreme position, the motion of the extreme waves is studied, showing the familiar nonlinear modification of the dispersion relation in the physical solution, and changes in the quadratic energy spectrum in second and higher order only. In section 3 we investigate what can be said about the maximal possible amplitude for signals obeying certain constraints. In particular we consider as constraints the simplest motion invariants of energy and momentum (constants during the

---

[1] Actually, in this paper we consider only the family with one pair of initial side bands: SFB(1); higher order families with n pairs of sidebands also exist, SFB(n). The case $n = 2$ shows phenomena like the interaction of two SFB(1) solutions, somewhat similar to interaction in NLS of two confined soliton wave groups .

down stream evolution), and show that the extreme signal has as remarkable property that it is a solution of a specific optimization principle. Remarks and conclusions about the relevance of the results obtained in this paper for more realistic situations will finish the paper.

2 Nonlinear modulation instability in the SFB family

This section is based to a considerable extent on the results presented in [2]; see this paper also for additional references. After some preliminaries, a global description of downstream running nonlinearly distorted waves according to SFB is presented, the extremal signal is studied, and the detailed dynamics near the extreme position is investigated.

2.1 Preliminaries

The explicit expression for the solution of the NLS equation called Soliton on Finite Background is given in [1]; we use the notation of [2]. The solution is given for the complex amplitude $A(\xi, \tau)$:

$$A\left(\xi, \tau\right) = r_0 e^{-i\gamma r_0^2 \xi} \left(\frac{\tilde{\nu}^2 \cosh\left(\sigma \xi\right) - i\tilde{\nu}\sqrt{2 - \tilde{\nu}^2}\sinh(\sigma \xi)}{\cosh\left(\sigma \xi\right) - \sqrt{1 - \tilde{\nu}^2/2}\cos\left(\nu \tau\right)} - 1 \right).$$

This describes actually a family of SFB solutions which depend on two essential parameters, r_0 and ν; two other parameters are related to a shift in time and position: we will choose these such that the extreme wave will appear for normalized variables at $x = 0$, with maximal height at $t = 0$.

The parameter r_0 denotes (half of) the amplitude of the uniform wavetrain at infinity, while $\tilde{\nu}$ is a normalization of the modulation frequency ν of the given carrier frequency. In fact, with the notation from [2], we have $\tilde{\nu} = \sqrt{\beta/\gamma}\nu/r_0$. Compared to the definition of Benjamin-Feir Index BFI in [6], adapted for the case considered here, we have the relation $\tilde{\nu} = \sqrt{2}/BFI$ so that Benjamin-Feir instability takes place for $\tilde{\nu} < \sqrt{2}$, corresponding to $BFI > 1$. The parameter $\sigma = \gamma r_0^2 \sqrt{2 - \tilde{\nu}^2}$ happens to be the Benjamin-Feir growth factor of linear instability theory.

In the following we will use the notation SFB to denote the solution in physical variables, describing the surface elevation $\eta(x, t)$ of the physical waves without the second order Stokes effect. These second order effects can be added; they will contribute to the actual wave heights, and show modulations (with double modulation frequency) on the MTA described below, but will not essentially contribute to the basic phenomenon. The role of the second order effects in generating four wave interaction and resonance phenomenon is already accounted for (in the considered order of accuracy) by the NLS equation. Another important consequence of this is that in the following we deal mainly with the wave amplitudes which directly determine the waveheight as twice the amplitude.

In the following we will consider the spatial NLS-equation, in which case the SFB will be periodic in time, and soliton-like in the spatial direction, describing the spatial evolution of downstream running time-modulated waves.

For the deterministic SFB wavefield the significant waveheight H_s, a quantity that is fundamental in the statistical description of wave fields cannot well be defined. Yet, since the space asymptotics of the wave field is a uniform wavetrain, when considering the averaged amplitude of the one-third highest waves, the only consistent similar quantity would be the value $2r_0$. Adopting then the (seemingly arbitrary, but often used) definition of 'rogue' wave as waves of wave height larger then $2.2 * H_s$, this will give a rough idea in which cases in the following we are dealing with extreme waves.

2.2 Characteristic spatial evolution
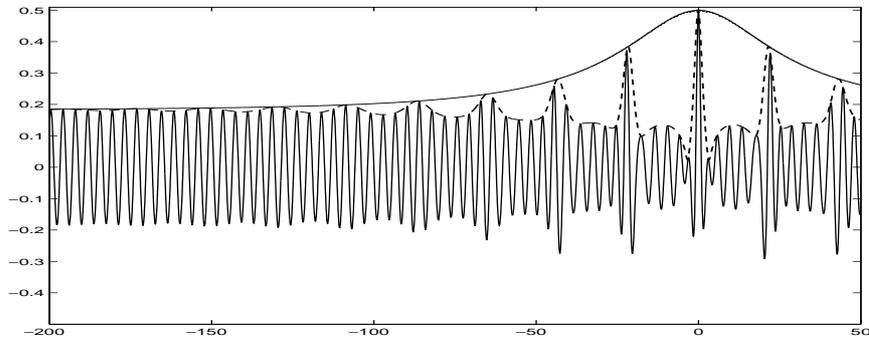
Fig. 1. Snapshot of the spatial wavefield SFB for $\tilde{\nu} = \sqrt{1/2}$. Shown are the individual waves, their envelope at that instant, and the time-independent MTA, maximal temporal amplitude. Physical dimensions are given along the axis: horizontally the distance and vertically the surface elevation in meters, for waves on a layer with depth of 5 meter.

Fig. 1 shows a plot of a snapshot of the spatial wavefield of waves running from left to right. At the left the slightly modulated uniform wave train (amplitude $2r_0$) is seen. This modulation clearly determines a characteristic modulation length that is maintained during the complete downstream evolution. While moving to the right, the modulations are amplified, creating distinct wave groups. At a certain position, called the *extreme position* (in scaled variables taken to be at $x = 0$), the largest wave appears, after which the reverse process sets in the decay towards the asymptotic harmonic wave train (with some phase change). Note that near the extreme position, the extreme wave is locally surrounded by waves of much smaller amplitude, as if the total energy in one wavegroup is conserved but with the energy redistributed between waves. In time, both

the waves and the envelope shifts to the right at different speed (the phase and group velocity respectively). Also shown in the plot is the so-called MTA, the *maximal temporal amplitude*: this is the (time-independent) curve determined by the maximal wave height at each point, the steady envelope of the wavegroups. Among other things, the MTA shows the global amplification factor, the ratio of the maximal and the asymptotic amplitude; this ratio is maximal 3, depending on $\tilde{\nu}$, but the local amplification factor near the extreme position can actually be much larger.

As is visible in Fig.1, the waves as they are running downstream, undergo increasingly large oscillations in amplitude. At a fixed position the maximal amplitude is given by the value of MTA, which is reached once every time period $T = 2\pi/\nu$. In between these successive maxima, the amplitude may be monotone, or (for sufficiently small values of $\tilde{\nu}$), non-monotone as is shown near the extreme position.
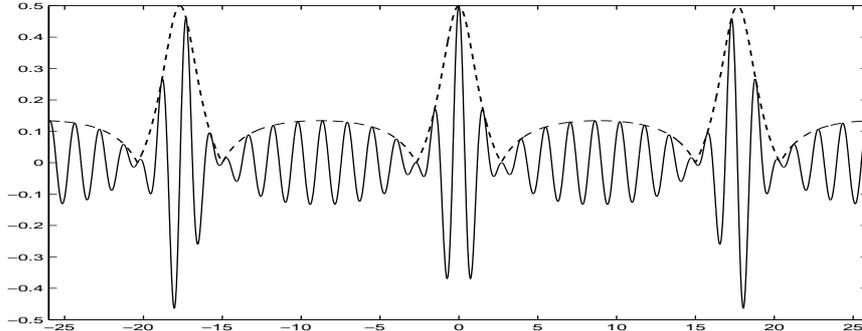
2.3 The extreme signal

The *extreme signal*, the time signal at the extreme position, has various special properties; we will denote the envelope by $S(\tau)$. First, this extreme signal is real, and its envelope is strictly positive for $\tilde{\nu} > \tilde{\nu}_{crit}$, while for $\tilde{\nu} < \tilde{\nu}_{crit}$ the envelope changes sign; here $\tilde{\nu}_{crit} = \sqrt{3/2}$. At times when the envelope vanishes, the phase experiences a π-jump, causing phase singularities. In any case we observe that at the extreme position all modes that make up the time signal are strongly phase correlated: either all having the same phase or some having opposite phase. More particularly, it was shown in [2] that the envelope S satisfies a Newton-type of equation and allows a simple phase-plane representation. Explicitly, the equation reads

$$\beta \partial_\tau^2 S + \gamma S^3 = \kappa S + \lambda \tag{1}$$

where κ, λ are positive constants (depending on $\tilde{\nu}$ and r_0). We will show in the next section that this is related to an optimization property.

For a characteristic value of $\tilde{\nu} < \tilde{\nu}_{crit}$, the time signal is plotted in Fig.2. We see that in one modulation period the wavegroup has been split in extreme waves and a number of intermittent waves of much smaller amplitude. The separation at times of a phase singularity, causes the intermittent and extreme waves to have opposite phase. In the spatial plot this shows itself in wave annihilation and wave creation at the successive singularities (see [2] for more details).

At the critical value $\tilde{\nu}_{crit} = \sqrt{3/2}$ for which the envelope vanishes at one point and is positive at the other times in the modulation period, the global amplification factor is precisely 2. To satisfy the 'rogue wave' definition of amplification larger than 2.2. the value of $\tilde{\nu}$ has to be smaller, i.e. will always correspond to the case when phase singularities are present; for instance, for $\tilde{\nu} = 1$, the amplification is $1 + \sqrt{2} \approx 2.4$.

Fig. 2. The extreme signal, i.e. the time signal at the extreme position where the largest waves appear. For the same SFB parameters and scaling as in Fig.1 the horizontal axis is the time in seconds.

2.4 Spectral properties of the extreme signal

The spectral description of the time signal at a fixed position is for the asymptotic modulated wavetrain according to Benjamin-Feir instability: the major part of the energy in the central frequency and small contributions in one pair of sidebands. As is to be expected form the change of the spatial envelope, an increase of the number of relevant sidebands and large energy exchange between the modes takes place while approaching the extremal position; depending on the value of $\tilde{\nu}$ the energy of the central frequency may have been transferred to neighbouring sidebands, for $\tilde{\nu} = \sqrt{1/2}$ even completely.

Actually, the appearance in the extreme signal of the phase singularities, and the corresponding partitioning of the waves within one modulation period in extreme and intermittent waves, causes that large differences in the spectrum are observed while practically the same envelope for the extreme waves is obtained. The intermittent waves 'modulate' the spectral properties of the extreme waves. This can be seen by writing the envelope $S(t)$ in one period $[0, T_{mod}]$ as the sum of an envelope $f(t)$ of the extreme waves, and an envelope $g(t - T_{mod}/2)$ of the intermittent waves centered at $T_{mod}/2 = \pi/\nu$. Then the spectral Fourier components of the complete envelope $S(t) = f(t) - g(t - T_{mod}/2)$, the minus-sign to indicate the π-phase difference between the waves, are given by $S_m = \hat{f}_m - (-1)^m \hat{g}_m$, with $\hat{f}_m, \hat{g}_m$ the spectral components of f and g in the m-th sideband respectively. The factor $(-1)^m = \exp(im\nu T_{mod}/2)$ is a consequence of the timeshift and has the modulational effect of decreasing and increasing the contributions in successive sidebands, starting with a decrease of the energy at the center frequency. In case the intermittent waves are such that $\Sigma |S_m|^2 < \Sigma \left|\hat{f}_m\right|^2$ this indicates that the presence of the intermittent waves makes it possible that the same maximal amplitude can be obtained for less energy. In Fig. 3 the spectra of the extreme signal are shown for three values of $\tilde{\nu}$.
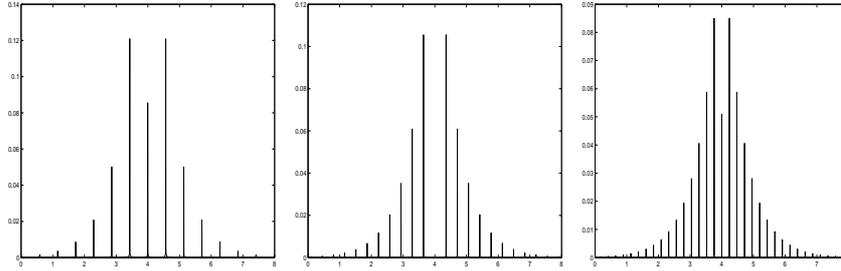
Fig. 3. The absolute value of the amplitude spectrum of the extreme signal for three values of $\tilde{\nu} = 1, \sqrt{1/2}, 1/2$ from left to right. Observe the vanishing contribution at the central frequency $\omega_0 = 4$ for $\tilde{\nu} = \sqrt{1/2}$.

The observation described here may be a warning when interpreting spectra for extreme waves, and just as well when looking for conditions on spectra to describe extreme waves. When background waves are present (the intermittent waves in the extreme signal may be considered like that), they will greatly disturb the spectrum related to the extreme waves and can increase the maximal possible amplitude at given energy.

2.5 Local evolution near the extreme position

We investigate the evolution of the signal and its spectral components in space near the extreme position. We show that the first order change in phase is described by a nonlinear modification of the dispersion relation with an additional quadratic term and a term of Fornberg-Whitham type. The change of the envelope, and of the quadratic spectrum, is shown to be of higher order.

The change of the amplitude near the extreme position is found from a direct Taylor expansion $A(\xi) = A(0) + \xi \left[\partial_\xi A\right]_{\xi=0} + \frac{\xi^2}{2} \left[\partial_\xi^2 A\right]_{\xi=0} + \ldots$. Using the evolution equation and the equation for S one gets

$$A(\xi) = S + i\xi(-\kappa S - \lambda) - \frac{\xi^2}{2} \left[2\gamma\kappa S^3 + 3\lambda\gamma S^2 + \kappa^2 S + \lambda\kappa\right] + O\left(\xi^3\right).$$

In the plane of the complex amplitude A, the evolution in time at $\xi = 0$ is on the real axis, crossing the origin if there is a phase singularity. For small ξ the solution above can be described as $A(\xi) = e^{-i\kappa\xi} S - i\xi\lambda + O\left(\xi^2\right)$ which has the geometric interpretation of two successive actions: the solution at $\xi = 0$ that lies on the real axis is rotated around the origin over an angle $-\kappa\xi$ and then followed by a shift along the imaginary axis over a distance $-\lambda\xi$.

For the absolute value of the NLS solution we find up to third order

$$|A(\xi)|^2 = S^2 - \xi^2 \left[2\gamma\kappa S^4 + 3\lambda\gamma S^3 - \kappa\lambda S - \lambda^2\right] + O\left(\xi^3\right),$$

while, writing $A = |A| e^{i\phi}$, the first order change of the phase ϕ at $\xi = 0$ is

$$\partial_\xi \phi = -\kappa - \lambda/S + O(\xi),$$

indicating once again the singular behaviour at the times of phase singularity where S vanishes. For the phase of the physical solution, $\psi = \phi + (k_0 x - \omega_0 t)$, this leads to $\partial_x \psi = k_0 - (\kappa + \lambda/S)$. Invoking the governing equation for S, the result for the local wavenumber can be written like

$$k(x) = k_0 - \left(\gamma S^2 + \frac{\beta \partial_t^2 S}{S} \right) + O(x).$$

This can be interpreted as a nonlinear modification of the linear dispersion relation with a quadratic contribution and a homogeneous term of Fornberg-Witham type.

For the Fourier transformation with respect to time, we denote the spectral components of $A(\xi)$ by $A_m(\xi)$ according to $A(\xi, \tau) = \Sigma A_m(\xi) e^{-im\nu\tau}$. Using the fact that S is real we find

$$A_m(\xi) = S_m + i\xi \left(-\kappa S_m - \hat{\lambda} \right) - \frac{\xi^2}{2} \left[2\gamma\kappa \left(\widehat{S^3} \right)_m + 3\gamma\lambda \left(\widehat{S^2} \right)_m + \kappa^2 S_m + \kappa\hat{\lambda} \right] + O(\xi^3).$$

Here $\hat{\lambda} = \lambda\delta(m)$ is a contribution to the central frequency $m = 0$ only, while $\widehat{S^2}$ and $\widehat{S^3}$ denote convolution of second and third order respectively. For the absolute value we find up to third order

$$|A_m(\xi)|^2 = S_m^2 - \xi^2 \left[2\gamma\kappa S_m \cdot \left(\widehat{S^3} \right)_m + 3\lambda\gamma S_m \cdot \left(\widehat{S^2} \right)_m - \kappa\hat{\lambda}S_0 - \hat{\lambda}^2 \right] + O(\xi^3).$$

To relate this with the change of the physical quadratic spectrum, we get for the quadratic spectrum using $\eta(x, t) = \Sigma A_m(x) \exp[-i(\omega_0 + m\nu)t] + cc$:

$$P_m(x) = P_m(0) - x^2 \left[2\gamma\kappa S_m \cdot \left(\widehat{S^3} \right)_m + 3\lambda\gamma S_m \cdot \left(\widehat{S^2} \right)_m - \kappa\hat{\lambda}S_0 - \hat{\lambda}^2 \right] + O(x^3).$$

Writing $A_m = |A_m| e^{i\theta_m(\xi)}$ we find at $\xi = 0$ for the phase change of the spectral components of the amplitude $\partial_\xi \theta_m(0) = -\kappa - \hat{\lambda}/S_0$. For the phase of the physical solution η this modifies the change due to linear dispersion:

$$\partial_x \psi_m = -\kappa - \frac{\hat{\lambda}}{S_0} + k_0 + m\nu/V_0,$$

which is the spectral version of the nonlinearly modified dispersion relation.

3   Extremal formulations

This section addresses some aspects centered around the question when a wave-field (or envelope) attains its maximal value, depending on the constraints that are imposed. We will denote this symbolically for a signal $s(t)$ like

$$\max_s \ \{\mathcal{A}\,(s) \,|\ \text{constraints}\ \} \ \text{with}\ \mathcal{A}\,(s) = \max_t s\,(t)$$

In particular, the effect of prescribing the quadratic spectrum is considered first. Then we consider the case of relevance for the evolution of waves, when we take as constraints motion invariants (integral quantities), and describe that the extreme signal of the SFB solutions of the previous section arises as special signal when the constraints are optimally chosen.

3.1 Constrained maximal signal amplitudes

Here we consider real functions of given period T and $\nu = 2\pi/T$, or look at signals with continuous spectrum (using the notation of the latter). Any signal with given quadratic spectrum $P(\omega)$ is of the form

$$s\,(t) = \int \sqrt{P\,(\omega)} e^{i\theta(\omega)} e^{-i\omega t} d\omega$$

for some phase function $\theta\,(\omega)$. A completely focussed signal would have all phases the same, say zero, $s_{foc}\,(t) = \int \sqrt{P\,(\omega)} e^{-i\omega t} d\omega$, and produces the signal that for the given quadratic spectrum has the largest amplitude (at $t = 0$), and

$$\max_s \ \{\mathcal{A}\,(s) \,|\ s \ \text{has given quadratic spectrum}\ P\,(\omega)\ \} = s_{foc}\,(0) = \int \sqrt{P\,(\omega)} d\omega.$$

If we relax the constraints, the results critically depend on the constraints. For instance, if not the spectrum, but only the value of the integrated quadratic spectrum is prescribed, the related maximization problem has no finite solution. In Fourier language this is related to the fact that the energy is equally partitioned over all sidebands: equipartition of energy. We indicated in the previous section that intermittent waves can partly contribute to a better equipartition. If stronger norms that the integrated quadratic spectrum are prescribed, finite solutions will exist.

Most relevant seems to consider the maximization problem with constraints that are motivated by physics. To that end we introduce the following functionals that are related respectively to the approximation of the physical energy H, the physical momentum I and the 'mass' functional M defined by

$$H\,(s) = \int_0^T \left[\frac{\beta}{2}\,(\partial_t s)^2 - \frac{\gamma}{4} s^4 \right] dt, \ \ I\,(s) = \int_0^T \frac{1}{2} s^2 dt, \ \ M\,(s) = \int_0^T s\,dt,$$

and we investigate the optimization problem[2]

$$\max_s \ \{\mathcal{A}\,(s) \,|\ H(s) = h;\ I(s) = g;\ M(s) = m\ \}. \tag{2}$$

---

[2] A very interesting statistically motivated variant of this maximization problem (without the linear mass-constraint) has been considered by Fedele [3]. He considers the initial value problem (evolution in time) and uses the Hamiltonian and quadratic invariant functionals that are related to the Zakharov equation, and takes as values of the constraints the values of a linearized wavefield at an initial time.

The resulting equation for (2) follows with Lagrange multiplier rule:

$$\sigma \delta \mathcal{A} = \lambda_1 \delta H + \lambda_2 \delta I + \lambda_3 \delta M \tag{3}$$

where we write the variational derivative of a functional K like δK (when equated to zero, $\delta K = 0$, this is precisely the Euler-Lagrange equation of the functional K). The multipliers are related to the values of the constraints; when the rhs doesn't vanish, the multiplier σ can be taken equal to one without restriction. Explicitly, the equation reads

$$\sigma \delta_{Dirac} \left(t - t_{\max}(s) \right) = \lambda_1 \left[-\beta \partial_t^2 s + \gamma s^3 \right] + \lambda_2 s + \lambda_3$$

where $t_{\max}(s)$ is the time at which s attains its maximum, and δ_{Dirac} denotes Dirac's delta function. When the rhs vanishes, which is consistent with $\sigma = 0$, we recover the equation for the extremal signal of SFB described above. This is only the case if the constraint values g, h, m are chosen correctly; we show in the next subsection that this holds for the extremal signal.

For non-optimal constraint values, the multipliers will be different and $\sigma \neq 0$. Then formally the extremal signal can still be found explicitly but will not be a realistic physical signal since it contains a discontinuity in the derivative at the time of maximal amplitude as a consequence of the delta-function; the optimal solution is then obtained by pasting continuously together parts of a suitable extreme time signal. Although the signal itself may be non-physical, its value of the maximal amplitude provides an upperbound for any other signal satisfying the constraints.

3.2 Extremal property of the extreme signal

As stated above, among signals that satisfy constrained values of the functionals H, I, M the ones with maximal amplitude will be obtained when the constraints are such that these three functionals are linearly related (when $\sigma = 0$). We will now show that the extremal signals have this property.

Indeed, for suitable parameters ν, r_0 related to the constraint values g, m, the extreme signal will be a solution of the constrained optimization problem for the physical energy

$$\min_S \left\{ H(S) \mid I(S) = g, \, M(S) = m \right\} \tag{4}$$

Indeed, an extremizer of this optimization problem satisfies the Lagrange multiplier formulation

$$\delta H(S) = -\kappa \delta I(S) - \lambda \tag{5}$$

for some multipliers $-\kappa, -\lambda$. Written in full for the specific functionals, this is precisely the Newton equation (1) for the extreme signal. Actually, using the fact that H and I are restrictions to real-valued amplitudes of motion invariants for the complex amplitude of NLS, these values in (4) are immediately found from the asymptotic values at the uniform wavetrain; we will describe this in more detail in a forth coming paper [4].

4 Conclusions and remarks

We have studied a special class of wavefields and extracted several properties that may be useful for the understanding of the appearance of extreme waves in more realistic situations.

Although the wavefields are derived from the simple NLS-model and no rigorous mathematical proof of their validity can be given, at least it can be said that these wavefields seem to be realizable in practice, as was shown by actual experiments performed in large wavetanks at MARIN, see the contribution of Huijsmans e.a. [5] in these proceedings. The experimental verification is vital, in particular because most simplified models (and certainly NLS as has been used here) do not predict breaking phenomena. When breaking occurs, the deterministic predictions become useless, while if no breaking occurs it can be expected that the predictions have qualitative, and as has been shown in the experiments, also quite good quantitative, validity.

It is also appropriate to discuss the validity, the 'robustness', of the basic phenomena described here for extension to more realistic situations. In particular this concerns the optimization property of the extreme signal: can we expect such a property to hold in more realistic situations, without relying on any conviction that also in those cases " ...... la nature agit selon quelque principe d'un maximum ou minimum." (Euler, 1746).

The optimization principle involves three functionals. Two of them have a clear physical meaning, although for NLS the complexified versions have to be considered. These are H, which is when complexified the Hamiltonian of NLS and is an approximation of the energy, and the quadratic functional I which in complex form is also an NLS invariant that can be interpreted for the real wavefields as the momentum. These functionals will also be present as invariants for reliable models that are more accurate than the NLS model, since the energy and momentum expressions are (approximations of) motion invariants for the full surface wave equations under the assumptions of non viscous fluid and translation symmetry. It can therefore be anticipated, or at least it can be hoped, that these two functionals will be relevant in any optimization principle for realistic large waves at the extreme position.

The major questionable point in the idea to generalize (4) is the role of the so-called 'mass' functional M that does not seem to correspond to a physically well understood invariant functional in more general situations. From its definition, $M(S)$ is seen to be precisely the square root of the energy in the central frequency, $M(S) = S_0$. It will be shown in [4] that this 'mass' turns up as a special case, valid only at the extreme position, in a variational principle that describes the complete SFB evolution as a relative equilibrium according to general Hamiltonian theory. That variational formulation depends on (the existence of) a higher order invariant functional, and this seems to be related to the special properties of the completely integrable NLS equation considered here. So the results presented here do not unambiguously support the idea that the optimization principle for the extreme signal can be expected to hold also in more

realistic cases. Yet it is tempting to look for such extremal formulations also in more realistic cases.

It may even be possible to investigate in a direct way the optimization principle for the extreme signal from experiments in a well-controlled laboratory environment. One possibility is to calculate the values of the relevant functionals from the measured signal at the extreme position, and investigate how close these values are near the optimal values from the minimizing property. Another, less robust (and therefore maybe more informative) method may be to use the fact that the extremizing property reflects itself in a simple phase-plane representation of the signal, see [2], so that the phase plane representation of the experimental extreme signals could give an indirect indication. Further research in this direction will be executed.

References

1. N.N. Akhmediev and A. Ankiewicz, *Solitons, Nonlinear pulses and beams*, Chapman & Hall, 1997

2. Andonowati, N. Karjanto and E. van Groesen, Extreme wave phenomena in downstream running modulated waves, submitted July 2004.

3. F. Fedele, The occurence of extreme wave crests and the nonlinear wave-wave interaction in random sea; *Proceedings XIV ISOPE Conference,* Toulon, France, May 2004..

4. E. van Groesen and Andonowati, Variational formulations for extreme waves, to be published.

5. R.H.M. Huijsmans, G. Klopman, N. Karjanto and Andonowati: Experiments on extreme wave generation based on Soliton on Finite Background; in *Proceedings 'Rogue Waves 2004'*, Brest France, October 2004.

6. P. Janssen, Nonlinear four-wave interaction and freak waves, *JPO* **33** (2003) 863-884